

Accepted Manuscript

Title: Role of surface synergistic effect on the performance of Ni-based hydrotalcite catalyst for highly efficient hydrogenation of furfural

Author: Marimuthu Manikandan Ashok Kumar Venugopal
Kandasamy Prabu Ratnesh Kumar Jha Raja Thirumalaiswamy



PII: S1381-1169(16)30085-1
DOI: <http://dx.doi.org/doi:10.1016/j.molcata.2016.03.019>
Reference: MOLCAA 9818

To appear in: *Journal of Molecular Catalysis A: Chemical*

Received date: 3-1-2016
Revised date: 4-3-2016
Accepted date: 5-3-2016

Please cite this article as: Marimuthu Manikandan, Ashok Kumar Venugopal, Kandasamy Prabu, Ratnesh Kumar Jha, Raja Thirumalaiswamy, Role of surface synergistic effect on the performance of Ni-based hydrotalcite catalyst for highly efficient hydrogenation of furfural, *Journal of Molecular Catalysis A: Chemical* <http://dx.doi.org/10.1016/j.molcata.2016.03.019>

This is a PDF file of an unedited manuscript that has been accepted for publication. As a service to our customers we are providing this early version of the manuscript. The manuscript will undergo copyediting, typesetting, and review of the resulting proof before it is published in its final form. Please note that during the production process errors may be discovered which could affect the content, and all legal disclaimers that apply to the journal pertain.

Role of surface synergistic effect on the performance of Ni-based hydrotalcite catalyst for highly efficient hydrogenation of furfural

*Marimuthu Manikandan, Ashok Kumar Venugopal, Kandasamy Prabu, Ratnesh Kumar Jha and Thirumalaiswamy Raja**

Catalysis & Inorganic Chemistry Division, CSIR-National Chemical Laboratory,

Dr. Homi Bhabha Road, Pune - 411 008, India. E-mail: t.raja@ncl.res.in

Fax: (+) 91-20-25902633, Tel: (+) 91-20-25902006.

AUTHOR INFORMATION

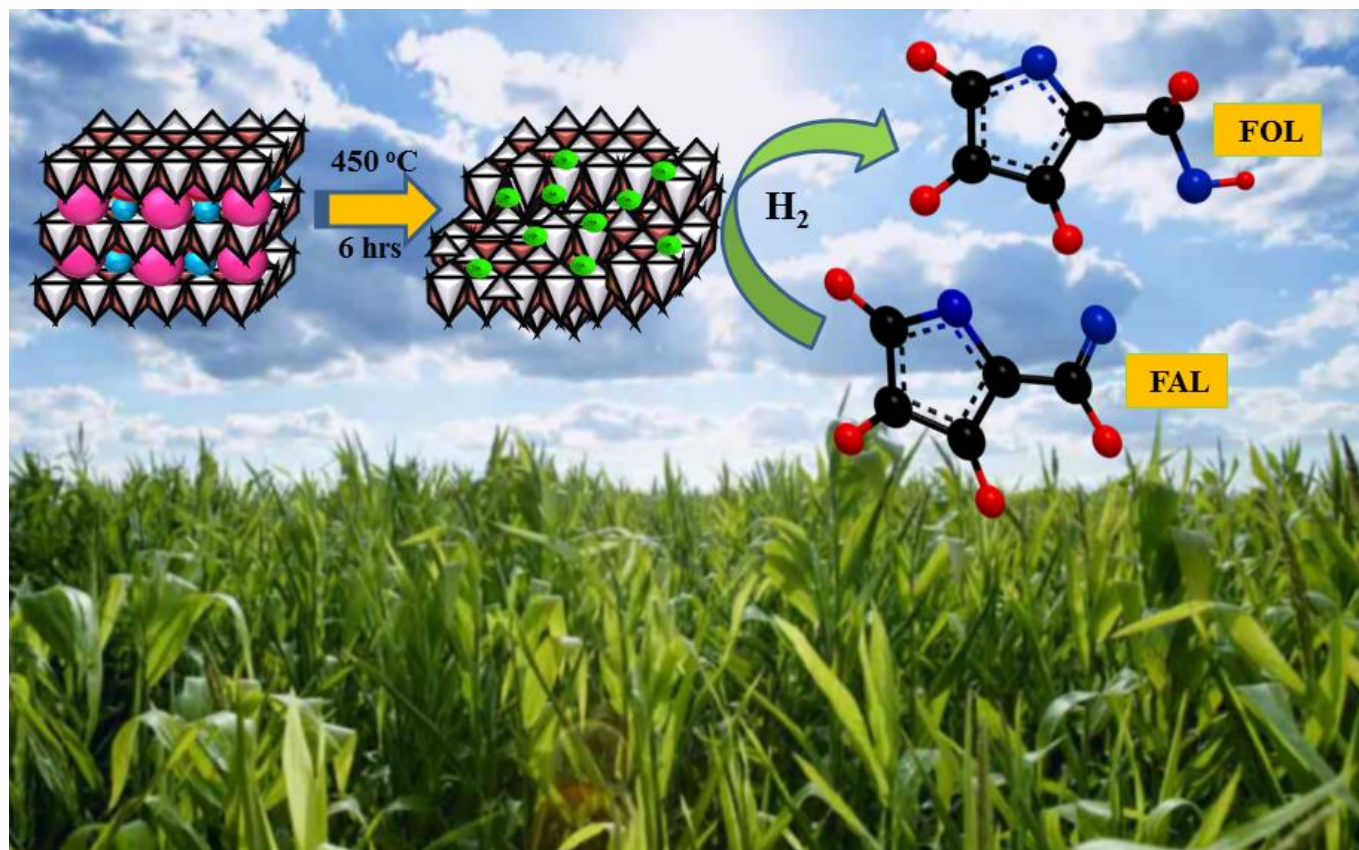
Corresponding Author

Thirumalaiswamy Raja*

Present Addresses

Catalysis & Inorganic Chemistry Division, CSIR-National Chemical Laboratory, Dr. Homi Bhabha Road, Pune- 411 008, India. E-mail: t.raja@ncl.res.in Fax: (+) 91-20-25902633, Tel: (+) 91-20-25902006.

Graphical abstract



Highlights

The selective vapour phase hydrogenation of furfural at ambient pressure has been investigated

The catalyst is a facile and robust hydrotalcite derived Ni containing mixed oxides

At optimized reaction conditions, furfural conversion of 98% with 95% of furfuryl alcohol selectivity was achieved

The results have demonstrated that the incorporation of Mg significantly enhances the Ni-support interaction, Ni dispersion and catalytic performance

The high efficiency of the Ni-based hydrotalcite derived catalyst was mainly attributed to the surface synergistic interaction between the catalytically active metallic Ni sites and the strong Mg (Al) O basic sites

The spent catalyst analysis substantiated that no significant difference in the catalyst phase was observed even after 48 hours of reaction stream.

ABSTRACT

The selective vapour phase hydrogenation of furfural at ambient pressure has been investigated using a facile and robust hydrotalcite derived Ni containing mixed oxide catalyst. The systematic characterization results conferred that the difficulty in the reduction of Ni species due to the strong interaction between Ni and support, which facilitated from the homogeneous distribution of hydrotalcite structure. It was also found that the structure and catalytic performance of the catalysts were greatly influenced by Ni loading. Through fine-tuned surface elemental sites and reaction conditions, furfural conversion of 98% with 95% of furfuryl alcohol selectivity was achieved over a MAN-2 catalyst containing two molar ratio of Ni. The results have demonstrated that the incorporation of Mg significantly enhances the Ni-support interaction, Ni dispersion and catalytic performance. The high efficiency of the Ni-based hydrotalcite derived catalyst was mainly attributed to the surface synergistic interaction between the catalytically active metallic Ni sites and the strong basic sites, which furnished an eco-benign and sustainable catalyst for the selective hydrogenation of furfural. Furthermore, the spent catalyst analysis substantiated that no significant difference in the catalyst phase was observed even after 48 hours of reaction stream.

ABBREVIATIONS

FAL, Furfural; FOL, Furfuryl alcohol; THFA, Tetrahydrofurfuryl alcohol; 2-MF, 2-methylfuran; THF, Tetrahydrofuran; 2-MTHF, 2-Methyltetrahydrofuran;

Keywords: Biomass-Furfural-Furfuryl alcohol-hydrotalcites-selective hydrogenation

1. INTRODUCTION

Owing to the increased need for energy, strict environmental benign concerns and continued depletion of fossil feedstock, the renewable energy resources have attracted an increased interest in all research sectors [1]. Recent efforts centered on the production of selected chemicals from biomass as an alternative and effective approach to replace fossil feedstocks. Lignocellulosic biomass is one of the low cost feedstocks, which is most abundant and bio-renewable resource on planet earth [2]. Biomass has been received an intense attention over the past few decades and many reports have been shown that lignocellulosic biomass has a great potential to be used as a renewable feedstock [2-4]. Hemicellulosic fractions of biomass have been used as feedstock to produce many important chemicals, such as furfural (FAL), furfuryl alcohol (FOL), tetrahydrofuran (THF) and furan etc., [5,6]. Among all, selective hydrogenation of biomass derived substrate is of great significance for future energy and fulfillment of fine chemical supply.

FAL is the most commonly available industrial chemical derived from hemicellulose, which is emerging to gain the attention of biofuel producers and academic researchers. Generally, FAL deserves a great advertence as a promising platform molecule for biofuels and non-petroleum based chemicals [7-9]. Among them, transformation of FAL to FOL has been considered as an important reaction due to its efficacy in various industries. Although it can be achieved by catalysis, there exists a strong interest for an effective heterogeneous catalyst that can operate selectively under milder and sustainable conditions. FOL is manufactured conventionally by the selective hydrogenation of FAL either in the gas phase or liquid phase [10-17]. In industry, the important platform molecule FOL is usually produced by vapor phase catalytic hydrogenation because of the large scale production and ease of operation. The most common industrial catalyst used for the process of FAL hydrogenation is Cr_2O_3 -promoted Cu-based ($\text{Cu-Cr}_2\text{O}_3$) with moderate activity at stringent reaction conditions. However it is not an eco-benign process due to the toxicity of Cr (VI) ions in the environment and human during catalyst preparation and testing [11]. To overcome these environmental problems, researchers have focused to develop an alternative and eco-benign Cr-free catalyst for the efficient production of FAL to FOL, which is more vital from the perspective of sustainable development of biomass resources and fuel-economy.

Over the past decades, the selective hydrogenation of FAL to FOL has been investigated in great numbers using Raney Ni, Ru, Pd, Cu supported metal catalysts and amorphous alloy catalyst with good performance.¹⁰⁻¹⁷ To the best of our knowledge, most of the reports revealed that the maximum yield of FOL was observed over copper in combination with other metals on various supports with severe reaction conditions. Nagaraja et al. reported the maximum yield (>98%) of FOL by using Cu/MgO and Cu-MgO-Cr₂O₃ catalysts [10,11]. Yan et al. achieved 95% of FOL yield using Cu-Cr catalyst at a high reaction temperature (120–220 °C) and hydrogen pressure (35–70 bar) [11]. However, the main disadvantages of the above catalysts are the reusability and non-ecological, due to its toxicity and severe deactivation of the active species within a short period of time. Moreover the effect of promoters in FAL hydrogenation also studied by different research groups [15]. Recently we have reported the promotional effect of Fe on Cu/ γ -Al₂O₃ catalyst for the efficient hydrogenation of FAL at ambient pressure [17]. Meanwhile, the utilization of noble metals for the selective conversion of FAL to FOL is also of great interest in recent days [12,13]. Kijeński *et al.* showed 87% of FAL conversion with 91% of FOL selectivity over Pt/TiO₂-V₂O₅-SiO₂ catalyst at vapor phase [12]. Fulajtárova *et al.* described the aqueous phase hydrogenation of FAL by using Pd-Cu catalysts with 98% of FOL selectivity [13]. Although, these catalysts showed superior performance, still it is far from satisfactory due to their cost and abundance that hampers towards commercialization.

Based on the reported literature, it is found that the developments of green and non-noble metal catalysts are crucial for the efficient production of FOL. Indeed, the focus on the alternate to the Cu-based systems also significant for developing the next generation catalyst. From the scientific viewpoint, the metal center that activates the hydrogen molecule can be used for the hydrogenation reactions. It is well known that a number of transition metals have been successfully investigated for the numerous hydrogenation reactions; especially Ni has been recognized as a promising candidate owing to its facile hydrogen activation. Sitthisa et al. reported a comparative study of hydrodeoxygenation of FAL by using Ni, Pd and Pt catalysts supported on SiO₂ and they concluded that Ni is more favorable for the ring opening products and the same group has shown Ni-Fe bimetallic catalysts for the production of 2-MF through hydrogenolysis [18]. Only a very few reports are available for the selective hydrogenation of FAL using Ni catalysts [19-21]. Most of the supported Ni catalysts showed activity towards a non-selective THFA instead of FOL due to its total hydrogenation ability [19]. There are no

impressive reports for selective hydrogenation of FAL to FOL by using Ni containing catalysts and all the available reports showed a maximum yield of THFA and ring opening products like butanal, butanol and butane [18]. Literature study revealed that Ni catalysts are seldom favorable for selective hydrogenation of FAL to FOL. The recent review reported by Nakagawa also substantiated the same [22]. Interestingly, this present work, hydrotalcite derived Ni containing mixed metal oxides showed good catalytic activity for selective hydrogenation of FAL to FOL under milder reaction conditions.

Hydrotalcite/Layered double hydroxides are synthetic or natural lamellar hydroxides with divalent and trivalent cations in the parent brucite type layer and different inorganic or organic anions in the interlayer. Usually, the necessary charge compensation (by substituting M^{3+} to M^{2+}) is achieved by planar carbonate ions intercalating between the brucitic layers. Also the additional anions, water molecules are located in the interlayer, occupying the remaining free space and connecting the hydroxyl groups of the brucitic layers through hydrogen bonding [23,24]. Upon calcination of the hydrotalcite-like (HTlc) compounds form mixed metal oxides that exhibit several significant catalytic properties such as high dispersion at the atomic level, small crystallite size, high thermal stability against sintering, large specific surface area and basicity [23-25]. Due to these specific characteristic properties, HTlc like compounds were widely used as catalyst for several reaction studies. In particular, Ni containing HTlc have been broadly investigated for the hydrogenation reactions, as it is economical and highly active [26,27]. In most cases Al_2O_3 is used for Ni catalysts as a support or in the hydrotalcite structure for various reactions. At the same time 'MgO' also used as a support for partial oxidation and reforming reactions [28,29]. Maa et al. reported that 'MgO' is an effective basic support for nickel catalysts for the suppression of coke deposition as well as higher nickel dispersion [30]. Strong interaction between 'Ni' and 'Mg' can promote the formation of 'Ni-Mg-O' solid solution, which led to the highest catalytic activity and stability [30,31]. In addition, it is widely known that the surface acid-base properties of catalysts may significantly influence the reaction progress. Recently, Liu et al. found that the surface basic sites on Cu-Mg-Al layered double hydroxide derived Cu-based catalysts could promote the catalytic performance in the hydrogenation of dimethyl 1,4-cyclohexane dicarboxylate (DMCD) and the same group has shown the surface synergism on Cu/MgO for FAL hydrogenation [12]. Based on these reports, we aimed to incorporate the 'MgO' in order to enhance the basicity of the NiAl-HTlc derived catalysts. Furthermore,

numerous catalytic studies of Mg/Al/Ni mixed oxides derived from HTlc like precursors were reported due to their good performance in various organic transformations [31-35]. Nevertheless, the selective FAL hydrogenation activity of the said catalyst is rarely reported.

Inspired by the above results, in this work, the efforts were made to synthesize a series of environment-friendly Mg-Al-Ni mixed metal oxides derived from HTlc-like precursors and deliberated their catalytic performances in the vapor phase selective hydrogenation of FAL to FOL at ambient pressure. In combination with systematic characterization, the influence of the Ni loading on the support interaction, metal dispersion, surface basicity and catalytic performance of the Mg/Al/Ni catalysts were elucidated. It was found that high conversion (97.6%) and selectivity to FOL (94.5%) was achieved over MAN-2. This could be attributed to the surface synergistic effect between the catalytically active metallic Ni species and the strong Mg (Al)O basic sites, which mainly held the cause of the hydrogenation reaction combined to the hydrogen dissociation and carbonyl group activation. More importantly, the obtained catalyst achieved a sustainable catalytic performance up to 48 hours without any deactivation. The activity and stability of Mg-Al-Ni catalysts were compared with those of NiAl-HTlc (takovite like) catalyst. Finally, the robustness of the catalyst was investigated by XRD, TGA along with the TEM characterization of the used samples, established no obvious change in structure and morphology. Our results demonstrate that the Ni-based hydrotalcite catalysts have significant potential for further development of biomass-derived substrates to value added chemicals.

2. EXPERIMENTAL SECTION

2.1. Materials.

All the chemicals were reagent grade and used without further purification. FAL (99%), FOL (99%), 2-MF (99%), THFA (99%), THF (98%), Furan (99%) were sourced from Sigma-Aldrich. Mg (NO₃)₂·6H₂O, Al (NO₃)₃·9H₂O and Ni (NO₃)₂·6H₂O, NaOH and Na₂CO₃ were purchased from Merck.

2.2. Catalyst synthesis.

Nickel containing HTlc derived mixed metal oxide catalysts (ratio of cations M²⁺/M³⁺=3: 1) was synthesized by modifying conventional co-precipitation method [36]. The synthesis procedure was as follows: A suitable molar ratio of metal precursor solution A was prepared by dissolving Mg (NO₃)₂·6H₂O, Al (NO₃)₃·9H₂O and Ni (NO₃)₂·6H₂O in 100 ml of distilled water. Precipitating agent solution B was prepared by dissolving NaOH and Na₂CO₃ in 100 ml distilled

water. The metal nitrate solution A and alkali solution B were added simultaneously drop by drop into a beaker containing distilled water and stirred continuously. The pH was maintained at 10 ± 0.2 and precipitated solution was stirred for an hour. The resulting slurry was transferred into a Teflon coated autoclave and the solution was hydrothermally treated at the $150\text{ }^\circ\text{C}$ for 12 hours without stirring, which is usually provided higher metal dispersion and strong interaction with support [12]. The obtained precipitate was filtered and washed several times with deionized water to remove excess of the base. Then, the sample was dried in an oven for 12 hours at $110\text{ }^\circ\text{C}$. Finally, the Mg-Al-Ni HTlc precursors were obtained. The obtained HTlc was simply calcined at $450\text{ }^\circ\text{C}$ for 6 hours with a heating rate of $2\text{ }^\circ\text{C min}^{-1}$. After this procedure, the obtained mixed metal oxides were reduced at $500\text{ }^\circ\text{C}$ for 2 hours in the presence of pure hydrogen (40 mL min^{-1}) with a heating rate of $2\text{ }^\circ\text{C min}^{-1}$. The Ni containing mixed metal oxides ($\text{Mg}_{3-x}\text{Al}_1\text{Ni}_x$) was prepared with different molar ratio of nickel ($x=0.5, 1, 1.5, 2, 2.5, 3$) and named as MAN-0.5, MAN-1, MAN-1.5, MAN-2, MAN-2.5 and AN-3 respectively, where MAN stands for magnesium, aluminum and nickel.

2.3. Characterization techniques

Thermal analysis of the synthesized materials was measured using Perkin Elmer Diamond's thermo gravimetric (TG) instrument. X-ray diffraction (XRD) data of synthesized powder materials were collected from PAN analytical X'pert Pro dual goniometer diffractometer. The amount of 'Ni' present in the samples was estimated by Inductively Coupled Plasma-Optical Emission Spectroscopy (ICP-OES, Spectro Arcos, FHS-12) analysis. Temperature Programmed Reduction (TPR) and Temperature programmed desorption of CO_2 (CO_2 -TPD) studies were carried out using a Micromeritics 2920 instrument with a TCD. The specific surface area, pore volume and average pore diameter of the materials were determined by nitrogen adsorption-desorption analysis at liquid nitrogen temperature (-196°C) using Autosorb 1C Quantachrome USA. The specific surface areas of the each sample were obtained using the multipoint Brunauer-Emmett-Teller (BET) method. Pore volume and pore size measurements are collected from Barret, Joyner and Halenda (BJH) pore size distribution Desorption analysis. Nickel core levels were studied with X-rayphotoelectron spectrometer (XPS) system from Prevac and equipped with VG Scienta monochromator (MX650) using Al Ka anode (1486.6 eV). A FEI TECNAI F30 electron microscope operating at 300 kV was used for recording high resolution transmission electron microscopy (HRTEM) of all the materials. Raman spectra were recorded

on a Horiba JY Lab RAM HR800 Raman spectrometer coupled with microscope in reflectance mode with 632.8 nm excitation laser sources and a spectral resolution of 0.3 cm^{-1} . The detailed experimental descriptions were given in the supporting information.

2.4. Catalyst testing

Hydrogenation of FAL is carried out in a vertical down flow fixed bed reactor at atmospheric pressure. The pelletized 1mL (~0.65g, size: 0.5-0.8mm) catalyst was placed at the center of the Inconel alloy reactor (390mm X 140mm) between two layers of ceramic beads and quartz wool. The catalyst was pre-reduced for 2 hours at 500 °C in the presence H₂ flow (99.99%, Gas Hourly Space Velocity, GHSV 2400 h⁻¹), which is controlled by Brooks (5850 S) make mass flow controller. After that, the reactor was cooled down to the desired reaction temperature in the presence of the same hydrogen flow. A suitable flow of distilled FAL (Sigma-Aldrich, 99.5%, Liquid Hourly Space Velocity, LHSV 1.2-2.4 h⁻¹) was fed continuously from the high precision isocratic syringe pump (Lab Alliance, Series II) and vaporized into the reactor, then H₂ flow was changed to 1800 GHSV h⁻¹. The products were condensed by chilled water and collected at regular time intervals. The collected liquid products were analyzed by Gas Chromatography (GC) (Varian-CP3800) with FID having HP-5 capillary column (30m×0.32mm×0.25 μ). The gaseous products were also analysed by online GC (Thermo Scientific Trace 1110) equipped with TCD having Porapak Q column. The obtained products were identified by comparison with the authentic samples and the quantification was carried out using the external standard method. Each product as well as FAL was calibrated with its standard at different concentrations. Carbon balances were ranged between 96 and 100% and all data points were obtained in duplicate with an error of $\pm 2\%$. The FAL conversion, FOL selectivity and product yield were calculated and defined as follows:

$$\text{FAL Conversion} = \frac{\text{FAL}_{\text{in}} - \text{FAL}_{\text{out}}}{\text{FAL}_{\text{in}}}$$

$$\text{FOL Selectivity} = \frac{\text{FOL}_{\text{out}}}{\text{FAL}_{\text{in}} - \text{FAL}_{\text{out}}}$$

$$\text{FOL yield} = \frac{\text{FAL Conversion} \times \text{FOL Selectivity}}{100}$$

3. RESULTS AND DISCUSSION

3.1 Characterization of the catalysts

Fig. 1a shows the XRD profiles of as synthesized Ni containing HTlc precursors. The similarity in the diffraction pattern with the characteristic patterns for HTlc-like layered structure demonstrating the HTlc precursors were successfully fabricated [30]. All sample exhibit sharp and symmetrical peaks for (003), (006), (110), and (113) planes as well as broad asymmetric peaks for (102), (105) and (108) planes with a little trace of other crystalline phases. The XRD patterns suggests no peaks attributable to NiO is present, however a little hump located nearly at 34.3° corresponds to NiO in higher Ni loadings ($x > 1.5$) evidenced that the Ni is located at layered structure. The interlayer distance, calculated from the reflection at 11.4° (d_{003}) is 0.77 nm, which is similar to the value reported by Maa [30] and Ogawa [38].

Fig. 1b represents XRD profiles of calcined samples along with NiO and Mg(Al)O as references. For all samples, absence of layered hydrotalcite features evidenced that the disintegration of layered structures to mixed metal oxides due to heat treatment. TGA analysis of as synthesized and calcined catalysts also proved the formation of stable mixed metal oxide after calcination treatment at 450°C , since no characteristic weight loss was observed after 400°C (Fig. S1, ESI). As shown in the Fig. 1b, the XRD reflections of the calcined samples located around 37.4° , 44.7° and 63.3° are attributed to NiO [JCPDS. No. 47-1049] and Ni-MgO [JCPDS.No.34-0410] which are overlapped each other as a consequence of its highly dispersive nature [30]. The reflections belonging to the Mg(Al)O periclase phase were seen predominantly and also it showed the same reflections as Ni containing catalysts, known to be similar reflection behavior of both NiO and Mg(Al)O [JCPDS. No. 4-829] at 44.7° and 63.3° , which prevent to identify the discrete NiO crystallites. In a given series of samples, the peaks for NiO intensified slightly with increasing the relative content of Ni, which clearly indicates that the dispersion of Ni decreased as the loading increases. Reason for the high dispersion of NiO is that the Ni^{2+} and Mg(Al)O were atomically distributed in the HTlc structure. Clause et al. reported that the Al-containing phases can strongly interact with NiO and could substantiate the NiO species for HTlc-derived materials [39]. The above results demonstrated that the successful formation of well-dispersed NiO phase held a strong interaction with periclase support. The XRD pattern of reduced MAN-2 catalyst is shown in the Fig. S2, ESI. The XRD reflections at 44.5° , 51.8° and 76.2° are belongs to the characteristics of metallic Ni (111), (200) and (220) respectively

(PDF#04-0850), in addition to the corresponding features for both NiMgO and periclase [39]. The average crystallite sizes of the metallic Ni particles was calculated using the Scherrer formula according to the Ni (200) diffraction is about 11.3 nm, which is accordance with TEM results.

Composition and textural properties of all catalysts are given in Table 1. The BET surface area of neat HTlc is 189 m²/g and the catalysts containing lower Ni content (x=0.5-1.5) show almost similar surface area. The most active MAN-2 catalyst shows a small increment in the surface area is about 191.6 m²/g as well as larger pore size (21.6 nm) and pore volume (0.95 cc/g). An increase in the surface area might be due to the generation of new surface adsorption sites facilitated from the high Ni dispersion along with the enhancement of pore size and pore volume. Furthermore, the decrease in the surface area of MAN-2.5 and AN-3 samples is attributed to the agglomeration of Ni species on the support and also further increment of Ni loadings likely lead to pore blockage as evidenced from the TEM micrograph of reduced MAN-2.5 sample (Fig. S3, ESI) [40]. N₂ adsorption-desorption isotherm plots for calcined catalysts are shown in Fig. S4a, ESI. In all cases, the plots are corresponding to type IV isotherm with almost similar hysteresis loops. Among all, catalyst MAN-2 shows the highest volume of adsorption (inset), which might be the reason for superior surface area of MAN-2 as compare to others. The pore size distribution of the calcined samples is also shown in Fig. S4b, the pores are falling within a uniform range of 15-22 nm. In all textural evolution MAN-2 sample show distinct behavior ascribed to the appropriate Ni/Mg ratio in the HTlc structure.

To determine the nature and chemical state of Ni and support species over the calcined samples, Raman experiment is performed (Fig. 2). The lattice vibration and bond strength of Ni with support have been explained by using pristine NiO as a reference (Fig. S5, ESI), which has predominant peak located nearly around 502 cm⁻¹. According to Ghule et al. crystalline NiO exhibits two types of peak at 460 and 500 cm⁻¹, while a characteristic band located at 600 cm⁻¹ is expected if NiAl₂O₄ spinels are formed [42]. However, a single broad peak around 570 cm⁻¹ was observed in our case for lower Ni loadings (x<1), which was deviated from the Raman bands of pure NiO and NiAl₂O₄. According to Pérez-Ramírez et al. the band around 550 cm⁻¹ can be assigned to the incorporation of surface NiO species into the subsurface of the alumina, which implies the strong interactions between NiO and support [40]. As shown in the Figure, for the increase of Ni loadings the peaks were shifted toward lower frequency and it becomes narrow. A

perceptible change was observed in high nickel content ($x=3$), thus the peak was shifted very close to pure NiO revealing the diminished in the NiO-Mg(Al)O interactions. The obtained results allow us to conclude that the catalyst containing least amount Ni has strong interaction with support and is decreased as Ni content increases. The strong interactions could stabilize the NiO particles through the homogeneous dispersion and inhibit the sintering of NiO, as evidenced from the XRD results [39].

To further investigate the NiO-support interaction and reduction characteristics of the samples, TPR experiments were performed. Generally, MgO and Mg(Al)O do not show any characteristic reduction behavior due to the deficiency of reducible species [23]. TPR profiles of all calcined samples are shown in Fig.3. All catalysts display a broad H₂ consumption peak in the temperature range of 480-780 °C assigned to a reduction of NiO phase to metallic Ni, which is higher than the reduction temperature of pure Ni [325 °C, inset]. As we discussed earlier, the increase in reduction temperature is might be due to the good dispersion or extent interaction with support and it is typical feature for HTlc derived materials [39]. Due to this strong interaction the reducibility of the Ni becomes more arduous as observed by the reduction temperature shifts to higher temperature region. TPR profile also illustrates, with the decrease in Ni loading, the peak shifted toward a higher temperature attributable to the strong interaction with support as well as higher Mg content [31]. It is clearly indicated that the lower Ni content or higher Mg content prone for higher reduction temperature due to the high dispersion or hindered Ni sites. Tichit et al. also suggested that the reducibility of the Ni decreases when the Mg content increases [43]. Careful analysis of TPR profile implies some more interesting insights; for Ni rich MAN-2.5 and AN-3 catalysts, a weak reduction peak was observed with a maximum at 327 °C which can be attributed to a reduction of NiO-segregated phase [43], since it is close to the value for reduction of pure NiO as previously commented. These results are consistent with the lower surface area for the MAN-2.5 and AN-3 catalysts. The Xray photoelectron spectroscopy (XPS) spectrums of calcined and reduced MAN-2 catalysts were given in the supporting information (Fig. S6), which are deconvoluted by peak fitting method by Shirley background. The peak with high intensity at 854.6 eV corresponds to Ni²⁺ in NiO, which is similar to the reported values [44] and a small peak at 856.3 eV is due to hydroxide impurities present as Ni(OH)₂. The spectrum also shows a satellite peak around 861 eV was due to shake up electrons. The Ni 2p core levels of reduced MAN-2 shows a peak centered at 852.1 eV is assigned to nickel

metallic species [45]. On the basis of the XPS results, it is found that the NiO is reduced to Ni⁰ during pretreatment.

The Ni metal dispersion and Ni surface area of the catalysts were investigated by H₂ chemisorption using freshly reduced sample. As shown in the Table 1, the Ni dispersion increased monotonically from 0.5 to 4.5% with Ni loading up to MAN-2, and then decreased to 3.9 % for MAN-2.5. As a result, the addition of a large amount of Ni is not helpful for the high dispersion owing to growth of metallic Ni crystallites. In contrast to the TPR results, here low Ni loaded sample shows very less (0.5%) dispersion is ascribed to the aggregation of metallic Ni particle rise to form large crystallites during high temperature reduction. Moreover, the calculated Ni surface area shows an increased trend with Ni loading up to AN-3, which evidences the availability surface Ni species. TEM micrographs of as synthesized, calcined and reduced MAN-2 catalysts are shown in Fig. 4. The as synthesized HTlc precursor (Fig .4a) shows a layered structure with some distorted hexagonal shape morphology (inset), which is consistent with our previous report [45]. Fig. 4b shows the TEM image of calcined MAN-2 catalyst, which appears with a distorted sheet like morphology and slightly porous in nature. This phenomenon is commonly observed in calcined HTlc type materials. HRTEM image of MAN-2 sample displays (Fig. 4c) the lattice fringe corresponds to NiO with 'd' spacing value of 2.07Å. The selected area electron diffraction (SAED) pattern (Fig. 4c inset) with well-defined electron diffraction spots confirms the presence of crystalline NiO. Fig. 4d presents TEM image of reduced MAN-2 catalyst, it can be noted that small Ni clusters that are highly dispersed on the support without any agglomeration (Fig. 4e). The calculated average Ni nanoparticle sizes were in 10.8 nm range (Fig. 4f), which is in accordance with the XRD results.

CO₂-TPD measurement was used to probe the surface basicity of the HTlc derived samples. As shown in Fig. 5, except AN-3, all samples exhibit two CO₂ desorption peaks, including medium Lewis basic sites located at 200-350 °C and strong Lewis basic sites centered at 450-650 °C, which are related to the Mg²⁺-O²⁻ ion pairs or Mg-O-Mg groups, and coordinatively unsaturated O²⁻ ions, respectively [12]. However, the Mg-free AN-3 sample does not show any characteristic desorption peak, indicative of the absence of basic sites. With the increase in Mg content, the CO₂ uptake is increased, indicating the increase of basic sites. According to a quantitative analysis on the densities of basic sites of the samples (Table 1), the densities of total basic sites decrease from 0.5 to 0.19 mmol g⁻¹ for MAN-0.5 to MAN-2.5. Liu *et al.* recently showed the SB

sites are more active for hydrogenation of FAL and DMCD to its corresponding alcohols [12]. The evaluated density of SB sites is decreased from 0.45 to 0.19 mmol g⁻¹ from MAN-0.5 to MAN-1.5, and then it increased to 0.24 mmol g⁻¹ for MAN-2 catalyst followed by gradual decrease for MAN-2.5 and AN-3. Moreover, a shift in the peak around 450-650 °C to a higher temperature was observed over the MAN-2 sample, revealing strong CO₂-catalyst interactions and enhanced basicity. Therefore, the shift towards the higher desorption temperature of CO₂ as a decrease in 'Mg' content was indicative of modification in strong support interactions in the MAN-2 sample. In another way, higher Mg content furnishes superior support interaction, but less surface Ni species, other case normalized surface Ni sites and basic sites were achieved by altering the Mg/Ni ratio and it reached in most extent for MAN-2.

3.2 Catalytic Activity in the vapor-phase hydrogenation of FAL

The performance of the catalysts with various Ni loadings was investigated to achieve the maximum yield of FOL. The catalytic activity and selectivity for FAL hydrogenation on different catalysts are listed in Table 2. For all catalysts, FOL is the predominant product along with side products, which is shown in Scheme 1. Differences in the catalytic activity of each catalyst were clearly observed, whereas the conversion and selectivity of the catalysts with various Ni loadings ($x=0.5$ to 3) are shown in Fig. 6. As shown in the Figure, the catalysts having a lower amount of Ni ($x=0.5$ and 1) show very less conversion and selectivity with rapid deactivation within short time. TPR profile illustrated that both catalysts need very high reduction temperatures for the generation of active Ni species, which usually favors sintering and suppress the active sites. Both conversion and selectivity were increased with increasing Ni loading up to MAN-2 catalyst ($x=2$). Then the activity decreases with a further increment of Ni, which might be due to the agglomeration of nickel particles. In another way, TPR and surface area analysis, segregation of NiO phase and lower surface area were observed for the Ni rich (MAN-2.5 and AN-3) samples might be responsible for this decline in activity. Among all the catalysts employed, MAN-2 gave a maximum FAL conversion about 97.6% with 94.5% selectivity towards FOL and the reason for this superior behavior was delineated in the characterization results. Catalyst AN-3, which is prepared without 'Mg' gave only 74% conversion and 81% selectivity and lost its activity very shortly (5 hours), indicates that the

addition of 'Mg' in the HTlc structure led to more enhanced catalytic activity and stability than those without magnesium [30].

As for the hydrogenation catalyzed by metallic Ni, one important key for the excellent catalytic activity is a large accessible Ni surface area, because a higher Ni surface area can supply more catalytically active sites for hydrogen dissociation and thus higher conversion as well high product selectivity. However, in our catalyst system, the change in the activity of the catalysts does not change monotonically with the metallic Ni surface area (Table 1). The AN-3 catalyst with the largest Ni surface area exhibits moderate catalytic performance with less stability. Interestingly, the MAN-2 catalyst with the largest SB sites showed superior conversion and selectivity compared to others, although the MAN-2 catalyst presents a moderate Ni surface area. Furthermore, MAN-2 exhibits higher catalytic activity than the MAN-2.5 and AN-3 catalysts with the larger Ni surface areas. To understand the superior performance of Ni containing mixed oxides derived from HTlc, reactions was performed with pure nickel oxide, Mg(Al)O and compared with a MAN-2 catalyst, which is shown in Fig. S7, ESI. The plain MgAl-HTlc shows very less conversion (~18%) and no selectivity towards FOL, the pre-treated pure NiO shows nearly 29% conversion and the selectivity slightly lesser than MAN-2 catalyst in the initial hours, followed by rapid deactivation. To understand the role of HTlc structure, Ni/MgAl-imp catalyst was prepared by conventional impregnation method and studied for the activity of FAL hydrogenation. Noted from Table 2 (entry 9), the catalytic efficiency of Ni/MgAl-imp is markedly lower than that of MAN-2 with the similar Ni content. From the activity comparison of these catalysts, MAN-2 provide excellent catalytic activity and the results were proved that the addition of 'Mg' improved the overall activity and resistant to sintering, whereas the metallic Ni centers navigated the FOL selectivity. From these observations MAN-2 has been considered as the best catalyst among all the catalysts employed in this study and it is used for the further catalytic evaluation studies.

The selective hydrogenation of FAL reaction was studied as a function of temperature from the range of 180-240 °C by using MAN-2 as a catalyst under reaction conditions of 1800 h⁻¹ GHSV of H₂ and 1.8 h⁻¹ LHSV of FAL and the product distribution results are depicted in Fig. 7 and Fig. S8, ESI. Reactions were employed initially a little above the boiling point of the FAL and further studied for regular temperature intervals. The best results were observed at 180 °C with good conversion (97.6%) and selectivity (94.5%) to FOL. For an increasing the temperature to

200 °C, the conversion of FAL increases, but a decrease in selectivity was observed because of the formation of side products like THFA and 2-MF. By further increment of temperature to 220 and 240 °C, the conversion increased to 100%, but the selectivity of FOL decreases to less than 46% (240 °C) and 30% (240 °C) because of reaction is favored for hydrogenolysis and decarbonylation to form 2-MF (18%) and furan (24%) respectively. Interestingly, other products 1,2 and 1,5 pentanediol (PED) was also observed at very high temperatures (>220 °C) with almost 10% selectivity. The increase in conversion as increasing reaction temperature implies that reaction was highly influenced by kinetics. Hence 180 °C was considered as an optimum reaction temperature for maximum yield of FOL.

In addition, the effect of space velocity of the reactants was also studied with different flow rate of the FAL and hydrogen. The effect of FAL flow was studied with different flow rate of FAL i.e. 1.2, 1.8 and 2.4 LHSV h⁻¹ to evaluate its effect on the conversion and selectivity of FOL, MAN-2 was employed as a catalyst with 1800 h⁻¹ GHSV of H₂ and the reaction was measured at 180 °C. As shown in Fig. 8, at a very low FAL flow (1.2 h⁻¹ LHSV) highest conversion was observed with less selectivity to FOL attributable to the high contact time, whereas the selectivity towards FOL decreased due to the over hydrogenation which lead to THFA and other side products. Among various flow rates of FAL, at LHSV 1.8 h⁻¹ shows better activity. This optimized FAL flow shows maximum activity which might be due to the appropriate residential time of reactant molecules over the catalyst and also it prevents FOL from over reduction as well as non-selective products. The increasing flow of FAL leads to less conversion (65%) due to the less contact time, but the selectivity was almost same as compared to other flow rates. Also at higher FAL flow the maximum coke formation was observed, which is evidenced in TGA analysis of spent catalysts.

Conversion of FAL and selectivity of FOL was investigated by varying the H₂ flow. The reactions were carried out with three different flow rates of H₂ (GHSV 900, 1800 and 2400 h⁻¹) over a MAN-2 catalyst with 1.8 h⁻¹ LHSV of FAL at 180 °C reaction temperature. Fig. 9 shows the effect of H₂ flow on catalytic activity. A minimum flow of H₂ (900 h⁻¹ GHSV) shows very good conversion, but less yield of FOL due to the higher contact time and the formation of side products. The gradual decrease in the conversion after a certain time period mainly attributed to the coke deposition. The H₂ flow of 1800 h⁻¹ GHSV gave maximum activity with 98% conversion and 95% selectivity to FOL, which might be due to the optimum amount of H₂ flow

to get more yield of FOL and also to avoid over reduction. Finally, H_2 flow of 3000 h^{-1} GHSV gave less conversion, but more or less same selectivity of FOL as compared to 1800 h^{-1} GHSV because of the insufficient contact time. The increased flow of hydrogen in the reaction mixture decreases the fugacity of FAL can account for the decreased conversion. Since it is an ambient pressure system the solubility of H_2 in the reaction mixture was excluded from the assumptions. There are no considerable changes in activity result by further increment of GHSV, which emphasizes the hydrogenation of FAL follows the pseudo-first order kinetics [8].

Based on the experimental and activity results, it was found that the metallic Ni species could be the catalytically active centers for the hydrogen activation, which led to high FOL selectivity. In addition, the surface basic sites, especially SB sites in close proximity with the metallic Ni sites, can easily interact with the π^* acceptor orbital of the C=O group to enhance the reactivity of the carbonyl group. Hence, a tentative mechanism is proposed to rationalize the experimentally observed structure-activity correlation that the synergistic interaction between the surface Ni^0 sites and SB sites over the HTlc derived catalysts which are responsible for the selective hydrogenation of FAL to FOL. Therefore, the facile adsorption of the C=O group on the surface basic sites of the catalyst forms an active intermediate that contain nucleophilic oxygen species. Consequently, the π -bond of C=O is activated on the basic sites followed by the facile addition of dissociated hydrogen on the surface Ni^0 sites. Finally, the carbonyl group is saturated by two hydrogen atoms from the surface Ni^0 sites and formed FOL molecule departs from the basic sites. As a result, in the present catalyst system, a uniform distribution of the Ni and Mg(Al)O species in the catalyst precursors facilitates the high dispersion of the active Ni^0 species, as well as the formation of strong interfacial contact between the active Ni nanoparticles and the Mg(Al)O support. Correspondingly, the conversion rate of the carbonyl compounds increased significantly due to the facile dissociation of the H_2 molecules on the catalytically active Ni^0 sites and activation of carbonyl groups by the adjacent basic sites. Especially, such formed surface synergistic effect between the metallic Ni species and the basic sites on the MAN-2 catalyst with the highest amount of basic sites and the appropriate amount of Ni^0 sites can efficiently improve the hydrogenation of the FAL. Besides, the efficiency of the MAN-2.5 and AN-3 catalysts mainly relies on its huge Ni surface area, since it showed relatively weaker surface basicity.

The sustainable catalytic activity is very significant for any catalyst to its practical applications. To underpin the robustness of the catalyst, the reaction was carried out for prolonged time on stream (TOS, 48 hours) over a MAN-2 catalyst under the optimized reaction conditions. Fig. S9 presents the hydrogenation performance of MAN-2 catalyst as a function of time. As shown in the figure, the MAN-2 catalyst exhibits stable activity for the selective hydrogenation of FAL up to 48 hours. However, a marginal decrease in activity for final hours can be attributed to the coke formation. The XRD analysis of the spent catalyst (Fig. S2, ESI) further confirms that no obvious structural change is observed in the MAN-2 catalyst even after 48 hours of reaction, also account for the sustainable catalytic activity.

To investigate the factor for deviation in the catalytic activity over different reaction temperature and space velocity of the reactants, the most active MAN-2 catalyst was thoroughly analyzed after 48 hours TOS. Generally, the loss of catalytic activity of metal-based catalysts can be attributed to surface modification, aggregation of metal particles and coke deposition from substrates [12]. From the post-reaction of TEM characterization results, it is noted that no structural transformation or aggregation of Ni nanoparticles was observed in the MAN-2 spent catalyst (Fig. S10). Hence, the amount of coke deposition was evaluated for various reaction conditions using the results from TGA analysis (Fig.10). The TGA profile shows two characteristic weight losses at different temperatures. The first weight loss was observed in the range of 250-420 °C which ascribed to the removal of coke on the catalyst surface. The second weight loss above 420 °C is considered as the coke deposition with different graphitization [34]. The following results were obtained from the TGA analysis i) maximum weight loss were observed for 2.4 LHSV h⁻¹ of FAL because of the increase in reactant flow causes more coke formation, at the same time minimum weight loss was observed at 1.2 LHSV h⁻¹ is accordance with good conversion at minimum flow of FAL, ii) maximum weight loss was obtained at higher temperatures (220 and 240 °C) compared to 180 °C, which confirms the conversion increases with increased reaction temperature, at the same time more conversion favors to the formation of more coke due to the decarbonylation and deposition of polymerized products. The moderate results were obtained from the optimized conditions of 1.8 h⁻¹ LHSV of FAL flow and 180 °C. Based on the above results it can be observed that high coke formation is due to high feed flow and high reaction temperature.

4. CONCLUSIONS

An eco-benign nickel containing hydrotalcite derived mixed metal oxides were synthesized by simple co-precipitation followed by hydrothermal treatment method and used for the selective hydrogenation of biomass-derived FAL to FOL. It was deduced that the catalyst containing strong basic sites and moderate Ni surface area exhibited superior catalytic performance, which could be tentatively ascribed to the surface synergistic effect between the surface basic sites and metallic nickel species. On the basis of the results of investigations, a plausible reaction mechanism was proposed. The surface basic sites favored the activation of substrate molecules, while the metallic Ni sites contributed to the dissociation of hydrogen. Moreover, the influence of various reaction parameters were extensively studied and stable catalytic activity for FAL to FOL was observed up to 48 hours TOS. The spent catalyst analysis showed no significant difference in catalyst phase even after longer reaction time, which emphasized that the presented catalyst system has great potential for biomass utilization. From both academic and industrial view points, this work is very significant to tailor a low-cost and highly efficient non Cr-based catalyst for the selective vapor phase hydrogenation of carbonyls to alcohols.

ASSOCIATED CONTENT

Structural characteristics and chemical composition of various catalysts, TGA, N₂ adsorption – desorption analysis, CO₂-TPD, *in situ* XPS analysis, selectivity of other products over different temperature on FAL conversion and FOLselectivity.

ACKNOWLEDGMENT

We are grateful to Dr.C.V.V. Satyanarayana and Dr.C.S. Gopinath CSIR-NCL, Pune for their valuable suggestions and timely help. TR thanks the Department of Science and Technology, India-SERB (no. SR/S1/PC-17/2011) and CSC0125 12 FYP for funding and MM thanks DST for fellowship.

REFERENCES

- [1] G.W. Huber, S. Iborra, A. Corma, *Chem. Rev.* 106 (2006) 4044-4098.
- [2] C. Somerville, H. Youngs, C. Taylor, S. C. Davis, S. P. Long, *Science*, 329(5993), (2010) 790–791.
- [3] E. Taarning, C.M.Osmundsen, X. B. Yang, B. Voss, S. I. Andersen, C. H. Christensen, *Energy Environ. Sci.*, 4(3), (2011) 793–804.
- [4] J. Ragauskas, C. K. Williams, B. H. Davison, G. Britovsek, J. Cairney, C. A. Eckert, Jr. W. J. Frederic, J. P. Hallett, D. J. Leak, C. L. Liotta, J. R. Mielenz, R. Murphy, R. Templer, T. Tschaplinski, *Science*, 311(2006) 484.
- [5] C. H. Zhou, X. Xia, C. X. Lin, D. S. Tonga and J. Beltramini, *Chem. Soc. Rev.*, 40 (2011) 5588–5617.
- [6] S. Dutta, S. De and B. Saha, *Catal. Sci. Technol.*, 2 (2012) 2025–2036.
- [7] J. P. Lange, E. V. D Heide, J. V Buijtenen, and R Price, *ChemSusChem*. 5 (2012) 150 – 166.
- [8] R. V. Sharma, U. Das, Ramaswami S and A. K. Dalai, *Appl. Catal A: Gen.* 454 (2013) 127–136.
- [9] W. Huang, H. Li, B. Zhu, Y. Feng, S. Wang and S. Zhang, *Ultrason. Sonochem.* 14 (2007) 67–74.
- [10] a) B.M. Nagaraja, V. Siva Kumar, V. Shasikala, A.H. Padmasri, B. Sreedhar, B. David Raju and K.S. Rama Rao, *Catal. Commun.* 4 (2003) 287–293. b) B.M. Nagaraja, A.H. Padmasri, B. David Raju and K.S. Rama Rao, *J. Mol. Catal. A: Chem.* 265 (2007) 90–97.
- [11] a) K. Yan, G. Wu, T. Lafleur, C. Jarvis, *Renew. Sust. Energ. Rev.*, 38, (2014) 663–676. b) B.J. Liu, L. H. Lu, B. C. Wang, T. X. Cai, I. Katsuyoshi, *Appl. Catal., A: Gen.*, 171, (1998) 117–122.
- [12] a) J. Kijenski, P. Winiarek, T. Paryjczak, A. Lewicki and A. Mikołajska, *Appl. Catal. A: Gen.* 233 (2002) 171–182. b) H. Liu, Q. Hu, G. Fan, L. Yang, F. Li, *Catal. Sci. Technol.*, 5, (2015) 3960. c) O. F. Aldosari, S. Iqbal, P. J. Miedziak, G. L. Brett, D. R. Jones, X.

- Liu, J. K. Edwards, D. J. Morgan, D. K. Knighta and G. J. Hutchings, *Catal. Sci. Technol.*, 6 (2016), 234-242.
- [13] a) K. Fulajtárova, T. Sotáka, M. Hronec, I. Vávra, E. Dobrocká, M. A. Omastová, *Appl. Catal. A: Gen.*, 502, (2015) 78–85. b) R. S. Rao, R. Terry K. Baker and M. A. Vannice, *Catal. Lett.* 60 (1999) 51-57. c) M. J. Tayle, L. J. Durndell, M. A. Issacs, C. M. A. Parlett, K. Wilson, A. F. Lee, G. Kuriyakau, *Appl. Catal. B: Env.*, 180 (2016) 580–585.
- [14] X. Chen, H. Li, H. Luo, M. Qiao and *Appl. Catal. A: Gen.* 233 (2002) 13–20.
- [15] H. Li, H. Luo, L. Zhuang, W. Dai and M. Qiao, *J. Mol. Catal. A: Chem.* 203 (2003) 267–275.
- [16] a) M.M. Villaverde, N.M. Bertero, T.F. Garetto and A.J. Marchi, *Catal. Today*. 213 (2013) 87– 92.
- [17] a) M. Manikandan, A. Venugopal, A. S. Nagpure, S. Chilukuri and T. Raja, *RSC Adv.*, 2016, 6, 3888. . b) J. Wu, Y. Shen, C. Liu, H. Wang, C. Geng and Z. Zhang, *Catal. Comm.* 6 (2005) 633–637.
- [18] a) S. Sitthisa, D. E. Resasco, *Catal. Lett.*, 141, (2011) 784–791. b) S. Sitthisa and D. E. Resasco, *Catal. Lett.* 141 (2011) 784–791. c) S. Sitthisa, W. An, D. E. Resasco, *J. Catal.*, 284 (2011) 90–101.
- [19] Y. Nakagawa, H. Nakazawa, H. Watanabe and K. Tomishige, *ChemCatChem.* 4 (2012) 1791 – 1797.
- [20] R. Khairi, S. Hara, T. Ichikuni and N. Shimazu, *Catal. Sci. Technol.* 2 (2012) 2139.
- [21] H. Li, S. Zhang and H. Luo, *Mater. Lett.* 58 (2004) 2741– 2746.
- [22] Y. Nakagawa, M. Tamura and K. Tomishige, *ACS Catal.* 3 (2013) 2655–2668.
- [23] F. Cavani, F. Trifiro and A. Vaccari, *Catal. Today*, 11 (1991) 173-301.
- [24] J. Santhanalakshmi and T. Raja, *Appl. Catal A: Gen.* 147 (1996) 69-80.

- [25] A. C. C. Rodriguesa, C. A. Henriquesb and J. L. F. Monteiroa, *Mater. Res.*, 6 (4) (2003) 563-568.
- [26] H. Zhu, M. Zhou, Z. Zeng, G. Xiao and R. Xiao, *Korean J. Chem. Eng.*, 31(4) (2014) 593-597.
- [27] V. Rives, F.M. Labajos, R. Trujillano, E. Romeo, C. Royo and A. Monzon, *Appl. Clay Sci.* 13 (1998) 363–379.
- [28] Y.G. Chen, K. Tomishige, K. Yokoyama and K. Fujimoto, *J. Catal.* 184 (1999) 479.
- [29] O. Yamazaki, K. Tomishige and K. Fujimoto, *Appl. Catal. A: Gen.* 136 (1996) 49-56.
- [30] M. Li, X. Wanga, S. Li, S. Wanga and X. Maa, *Int. J. Hydrogen. Energ.* 35 (2010) 6699 - 6708.
- [31] K. Schulze, W. Makowski, R. Chyz'y, R. Dziembaj and G. Geismar, *Appl. Clay Sci.* 18 (2001) 59–69.
- [32] K. Takehira, T. Shishido, P. Wang, T. Kosaka, and K. Takaki, *J. Catal.* 221(2004) 43–54.
- [33] T. Shishido, M. Sukenobu, H. Morioka, M. Kondo, Y. Wang, K. Takaki and K. Takehira, *Appl. Catal. A: Gen.* 223 (2002) 35–42.
- [34] F. Basile, G. Fornasari, E. Poluzzi and A. Vaccari, *Appl. Clay Sci.* 13 (1998) 329–345.
- [35] Y.Z. Chen, C.M. Hwang and C.W. Liaw, *Appl. Catal. A: Gen.* 169 (1998) 207-214.
- [36] M. Zhou, Z. Zeng, H. Zhu, G. Xiao and R. Xiao, *J. Energy Chem.* 23 (2014) 91–96.
- [37] K. Roy, C.P. Vinod and C.S. Gopinath, *J. Phys. Chem. C*, 117 (2013) 4717–4726.
- [38] M. Ogawa and H. Kaiho, *Langmuir*, 18(11) (2002) 4240-4242.
- [39] a) O. Clause, B. Rebours, E. Merlen, F. Trifiro and A. Vaccari, *J. Catal.*, 133 (1992), 231-246. b) X. Kong, R. Zheng, Y. Zhu, G. Ding, Y. Zhu, Y. W. Li, *Green Chem.*, 17, (2015) 2504-2514.

- [40] C. Scherdel, G. Reichenauer and M. Wiener, *Microporous Mesoporous Mater.* 132 (2010) 572–575.
- [41] J. Pérez-Ramírez, G. Mul, J. Moulijn, *Vib. Spectrosc.*, 27, (2001) 75–88.
- [42] V. Ghule, K. Ghule, S.-H. Tzing, T. H. Punde, H. Chang and Y. C. Ling, *J. Solid State Chem.*, 182, (2009) 3406–3411.
- [43] a) D. Tichit, F. Medina, B. Coq and R. Dutartre, *Appl. Catal. A* 159 (1997) 241–258. b) O. W. Perez-Lopez, A. Senger, N. R. Marcilio, M. A. Lansarin, *Appl. Catal. A: Gen.*, 303 (2006) 234–244.
- [44] a) D. Addaria, A. Mignani, E. Scavetta, D. Tonelli and A. Rossia, *Surf. Interface Anal.* 2011, 43, 816–822. b) K. Domen, A. Kudo and T. Onish, *J. Phys. Chem.* 90 (1986) 293.
- [45] A. Romero, M. Jobbagy, M. Laborde, G. Baronetti, and N. Amadeo. *Catal. Today.* 149 (2010) 407–412.
- [46] V. Ashok Kumar, T.V. Aswathy, K. Periyasamy and T. Raja, *Green Chem.* 15 (2013) 3259–3267.

FIGURES

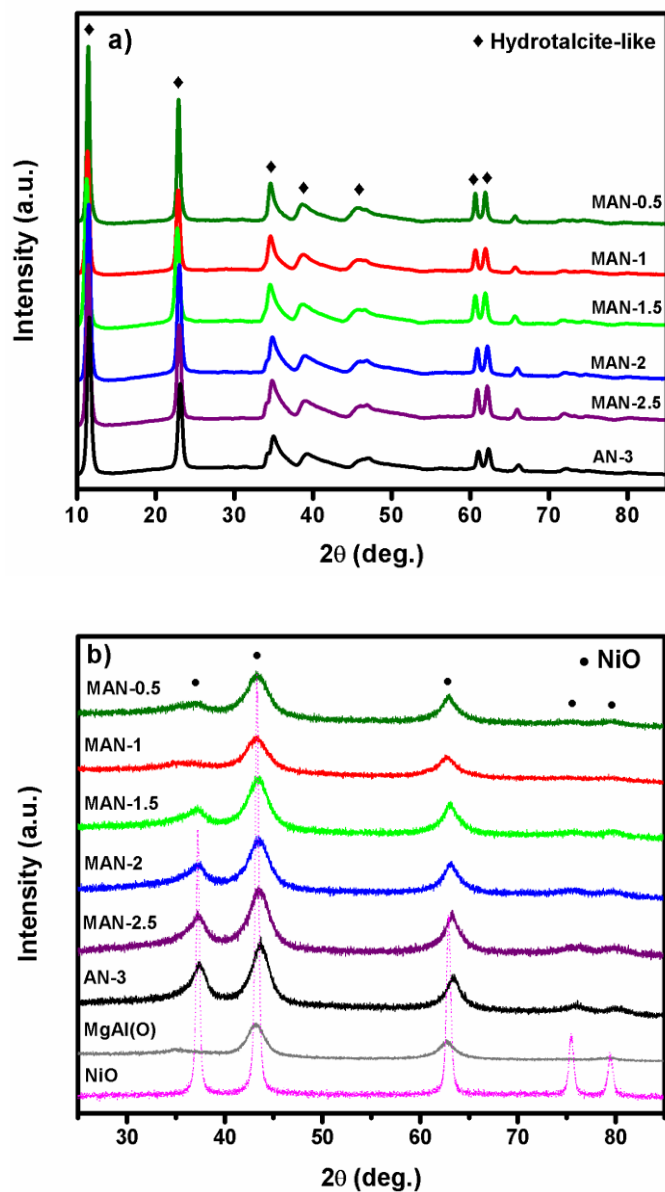


Fig. 1 XRD patterns of (a) uncalcined and (b) calcined hydrotalcite precursors. XRD results of NiO and Mg(Al)O are given for comparison.

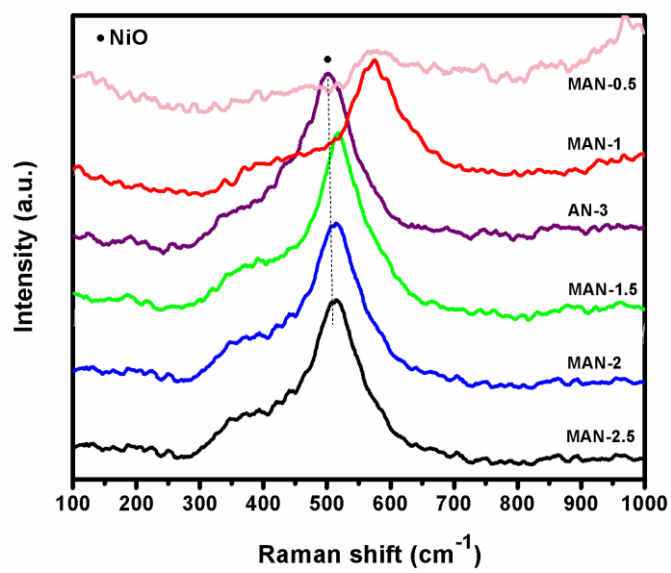


Fig. 2 Raman profiles of calcined hydrotalcite derived samples.

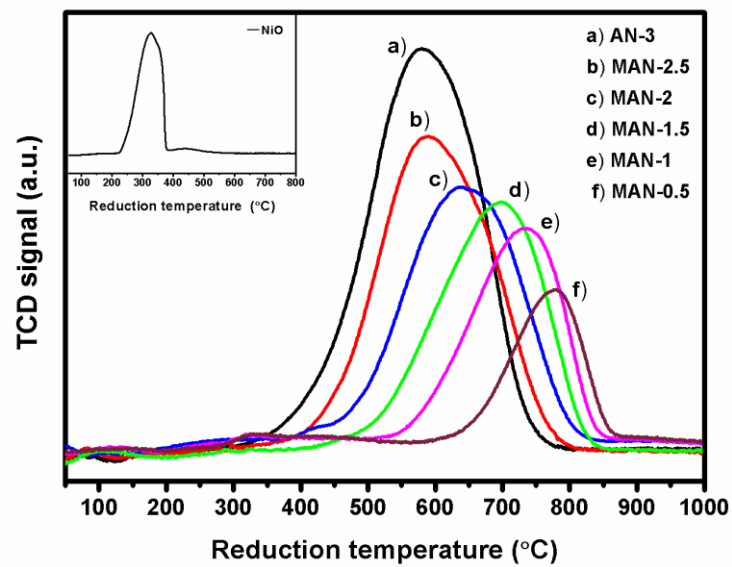


Fig. 3 TPR profiles of calcined hydrotalcite derived samples with NiO (inset) as a reference.

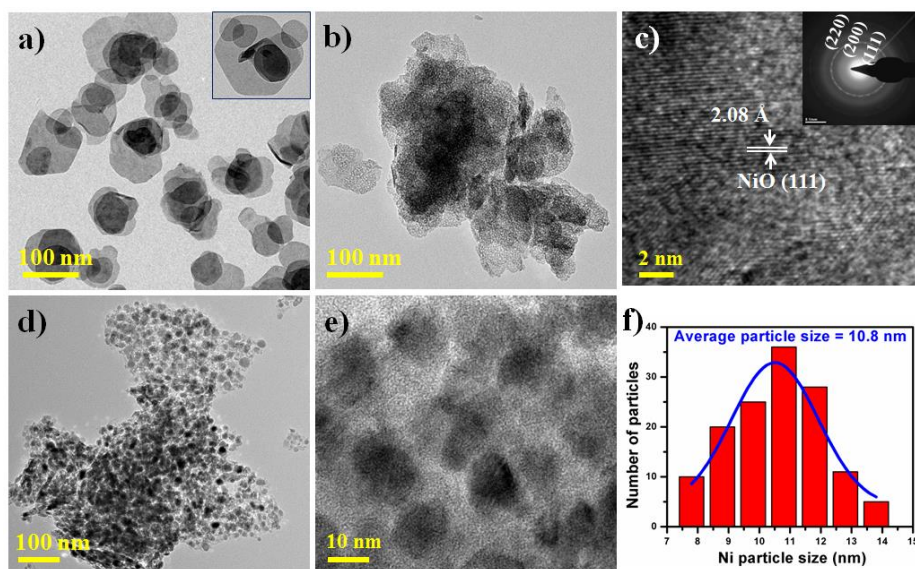


Fig. 4 TEM images of as synthesized (a), calcined (b&c) and reduced (d-f) MAN-2 catalysts.

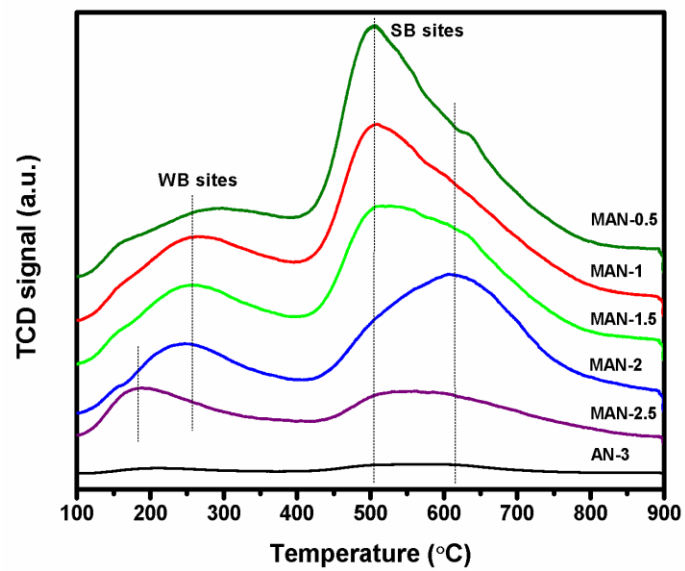


Fig. 5 CO₂-TPD of the different hydrotalcite derived samples after reduction.

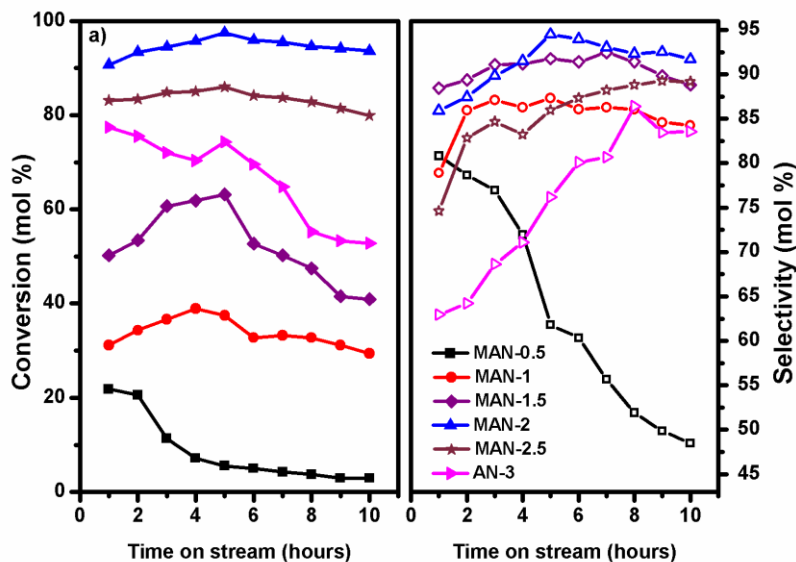


Fig. 6 a) Conversion of FAL and b) selectivity of FOL at various nickel loadings. Reaction conditions: 180 °C, LHSV 1.8 h⁻¹ with respect to FAL and GHSV 1800 h⁻¹ with respect to H₂, 1 atm. pressure and 1 mL catalyst. Solid closed symbols are used for the conversion and solid opened symbols are used for selectivity.

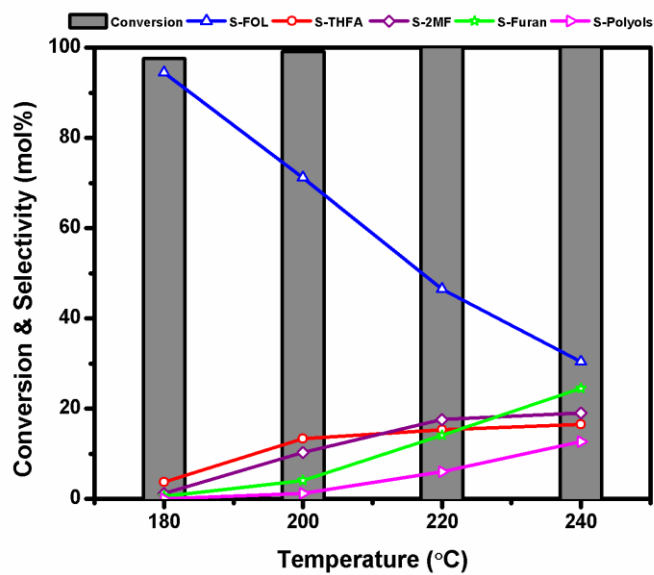


Fig. 7 Conversion of FAL and selectivity of different products at various reaction temperatures over MAN-2 catalyst. Reaction conditions: LHSV 1.8 h^{-1} with respect to FAL and GHSV, 1800 h^{-1} with respect to H_2 , 1 atm. pressure and 1 mL catalyst. Bar patterns are used for the conversion and solid opened symbols are used for selectivity (S).

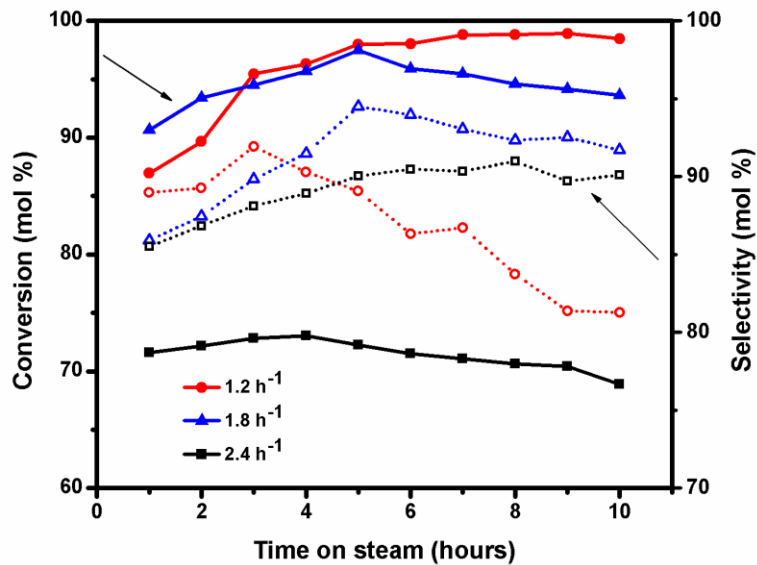


Fig. 8 Conversion of FAL and selectivity of FOL at different FAL flow rates over MAN-2 catalyst. Reaction conditions: 180 °C, GHSV 1800 h⁻¹ with respect to H₂, 1 atm. pressure and 1 mL catalyst. Solid closed symbols are used for the conversion and solid opened symbols are used for selectivity.

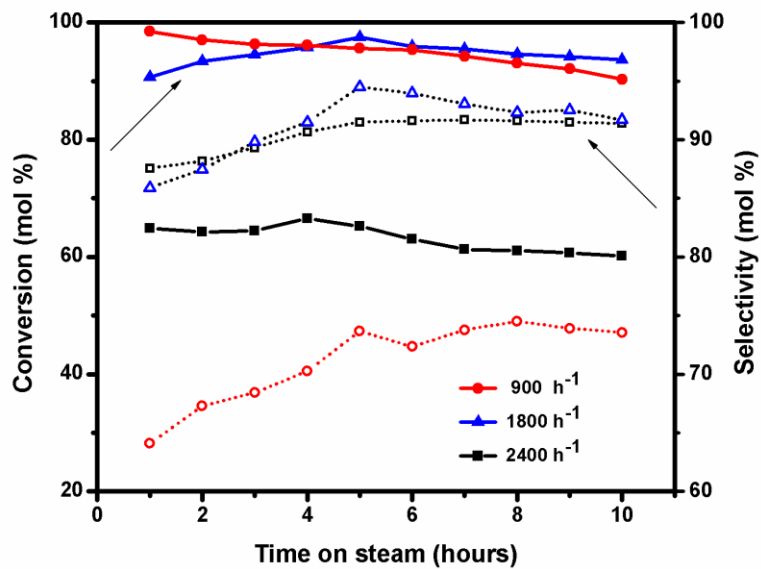


Fig. 9 Conversion of FAL and selectivity of FOL at different hydrogen flow rates over MAN-2 catalyst. Reaction conditions: 180 °C, LHSV 1.8 h⁻¹ with respect to FAL, 1 atm. pressure, 1 mL catalyst. Solid closed symbols are used for the conversion and solid opened symbols are used for selectivity.

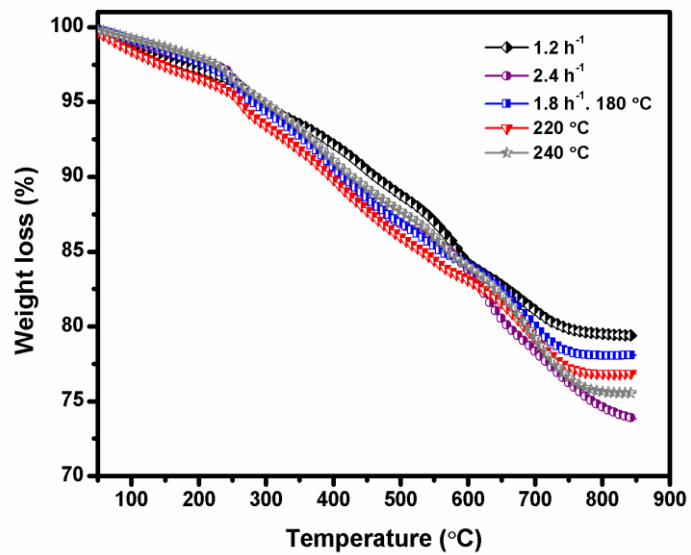
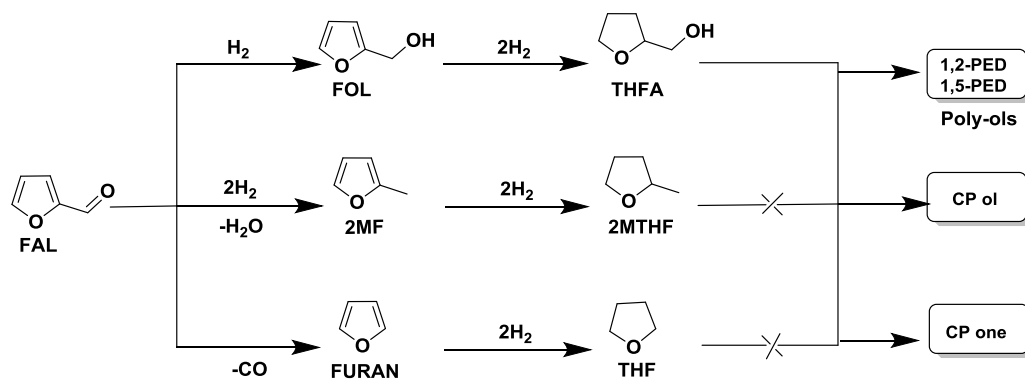


Fig. 10 TGA profiles of the MAN-2 spent catalysts at various reaction temperatures and FAL flow conditions.

SCHEMES



Scheme 1. Reaction pathway for the hydrogenation of FAL to FOL and other possible products.

Table 1. The structural and textural data of the different hydrotalcite derived samples.

S.No	Sample	Nickel ^[a] (wt %)	Surface Area ^[b] (m ² g ⁻¹)	Average pore diameter ^[c] (nm)	Total pore volume ^[c] (cc/g)	D _{Ni} ^[d] (%)	S _{Ni} ^[d] (m ² g ⁻¹)	Basic sites ^[e] (mmol g ⁻¹)	
								Total	SB sites
1	Mg(Al)O	---	189.0	---	---	---	---	0.523	0.48
2	MAN-0.5	18.1	166.8	19.2	0.79	0.5	1.2	0.50	0.47
3	MAN-1	30.4	163.5	18.5	0.63	1.3	2.47	0.48	0.38
4	MAN-1.5	43.4	165.8	14.0	0.58	4.1	12.9	0.47	0.19
5	MAN-2	48.3	191.6	21.6	0.95	4.5	13.6	0.36	0.24
6	MAN-2.5	60.3	175.7	17.8	0.78	3.9	15.2	0.18	0.11
7	AN-3	56.4	138.0	15.2	0.67	5.9	23.7	0.03	0.02

^[a] Amount of nickel was obtained from ICP-OES analysis ^[b] Obtained by BET surface area analysis ^[c] Calculated from BJH pore size analysis ^[d] D_{Ni}= Ni dispersion, S_{Ni}= Ni surface area, calculated from H₂-chemisorption experiments ^[e] Obtained by CO₂-TPD experiments

Table. 2 The catalytic performance of the different catalysts in vapor phase hydrogenation of FAL.^[a]

S.No	Catalyst (Mg:Al:Ni mole ratio)	Maximum Conversion (mol %)	Selectivity (mol %)				Yield of FOL (mol %)	Carbon balance ^[d] (%)
			FOL	THFA	Decarbonylation products ^[b]	Others ^[c]		
1	MgAl (O)	18.3	---	---	34	58.5 ^[e]	---	---
2	MAN-0.5	20.4	61.8	5.2	18.1	14.9	12.6	96.8
3	MAN-1	38.9	83.7	6.4	4.6	5.3	32.5	98.9
4	MAN-1.5	63.2	89.8	5.2	2.4	2.6	56.7	99.4
5	MAN-2	97.6	94.5	3.9	1.30	0.2	92.2	99.5
6	MAN-2.5	86.0	85.9	9.6	3.5	2.0	73.9	99.4
7	AN-3	74.3	80.7	13.7	3.8	1.8	59.9	99.0
8	Ni/MgO	62.4	81.3	11.2	3.6	3.9	50.7	99.2
9	Ni/MgAl imp ^[f]	73.6	76.2	19.3	4.2	0.3	56.1	99.2

^[a] Reaction conditions: 180 °C, LHSV 1.8 h⁻¹ with respect to FAL and GHSV 1800 h⁻¹ with respect to H₂, 1 atm. pressure and 1 mL catalyst. ^[b] Furan, THF and CO. ^[c] 2-MF and 2-MTHF. ^[d] Carbon balance calculated based on the identified products. ^[e] Unknown products. ^[f] Prepared by the conventional impregnation method.